technische universität
dortmund

Arbeit zur Erlangung des akademischen Grades
Bachelor of Science

Search for single top-quark production in the s-channel with the ATLAS experiment

Alfredo Manente
geboren in Dortmund

2025

Lehrstuhl für Experimentelle Physik IV
Fakultät Physik
Technische Universität Dortmund

Kurzfassung

In dieser Arbeit werden Studien zur Messung des Wirkungsquerschnitts für die Erzeugung einzelner Top-Quarks im s-Kanal bei Proton-Proton Kollisionen mit einer Schwerpunktsenergie von $\sqrt{s} = 13\,\text{TeV}$ durchgeführt. Die Daten stammen aus Kollisionsexperimenten des LHC und wurden vom ATLAS Detektor in den Jahren 2015 bis 2018 aufgenommen. Zur Extrahierung des Wirkungsquerschnitts wird ein Profile Likelihood Fit verwendet, wobei als Diskriminante die Ergebnisse eines *Deep Neural Networks*(DNN) fungieren. Die Signal Signatur besteht aus einem geladenen Lepton, entweder Elektron oder Myon, zwei b-tagged Jets und fehlendem transversalen Impuls.

Abstract

The abstract is a short summary of the thesis in English, together with the German summary it has to fit on this page.

Contents

1 Introduction

The Standard Model (SM) of particle physics is the best descriptor for the behaviour of elementary particles and the interactions between them. Despite its major successes, like the discovery of the Higgs boson (citation) or the top quark(citation), many phenomena remain unexplained. Physics beyond the Standard Model (BSM) is needed to make breakthroughs in dark matter, neutrino oscillations or the matter-antimatter disbalance.

As the heaviest fermion with a mass of about $172.5\,\mathrm{GeV}$ (citation?), the top quark is the strongest coupler with the Higgs field and may act as a potential probe for electroweak symmetry breaking. Therefore in it lies potential in uncovering BSM physics. The challenge lies in its short lifetime of $5 \times 10^{-25}\,\mathrm{s}$ (citation), which makes hadronisation impossible and almost exclusively leads to a W-boson and a bottom-quark as decay products.

At the ATLAS experiment of the Large Hadron Collider (LHC) top-quarks predominantly come in pairs of $t\bar{t}$ via the strong interaction. Although, top quarks can be produced singly via the electroweak interaction, with the single-top production in the s- and t-channel, as well as in tW associated production. The s-channel has the smallest cross section of $10.32\,\mathrm{pb}$ of all mentioned processes and is dominated heavily by background processes. Unlike the other single modes, the s-channel has not yet been measured precisely with a significance over 5σ, with the latest ATLAS measurement achieving an observed (expected) significance of 3.3(3.9). Even with its small cross section, the major hindrance in the measurement is the systematic uncertainties. To get a better measurement, this thesis will use a more modern approach, with a DNN output as the discriminant for a profile likelihood fit. Simulated data from proton-proton collisions in the LHC at $\sqrt{s} = 13\,\mathrm{TeV}$ corresponding to the full Run 2 dataset with a luminosity of $140\,\mathrm{fb}^{-1}$ from the ATLAS detector is used.

The structure of this work constitutes the following content. In chapter 2 an overview of the SM, the s-channel production mode as well as the dominant backgrounds and the previous measurement is given. Chapter 3 presents the ATLAS detector. Chapter 4 lists the samples, the object definitions and event selections used. Chapter 5 describes the main study presented in this thesis. Finally chapter 6 gives a short

summary of the results and an outlook for further advances in the measurement of the single top s-channel.

2 Properties of the Top Quark within the Standard Model

2.1 Overview of the Standard Model

The SM of particle physics is a gauge invariant theory, which describes the fundamental particles and the interactions between them. It was developed throughout the 20th century (citation) by combining the discoveries of quantum mechanics and special relativity into a quantum field theory. Three of the four fundamental forces, electromagnetism, the strong interaction and the weak interaction are characterized by it, only excluding gravity. Whereas electromagnetism and gravity act on infinite ranges, the strong and weak force act on subatomic scales.

The SM divides the fundamental particles into two main categories. First fermions, which constitute all known matter and carry half integer spin. Second bosons, which act out the interactions between fermions and carry a whole integer spin. Further, bosons can be divided into vector bosons, with spin 1 and a scalar boson, the Higgs boson (H) with spin 0. The fermions are comprised of quarks and leptons, where both interact with the electromagnetic (EM) force but only quarks experience the strong force. Neutrinos, which take part in the lepton category, only interact via the weak force. The fundamental particles are further split into three generations in relation to their masses and time of discovery. The first generation is comprised of the electron (e) and the corresponding electron neutrino (ν_e) for the lepton part, and the up quark (u) as well as the down quark (d). The second generation leptons include the muon (μ) and the muon neutrino (ν), while the charm quark (c) and the strange quark (s) constitute the second generation quarks. The third generation includes the heaviest fermions, with the tau lepton (τ) and its corresponding tau neutrino (ν_tau) on the lepton side and the top quark (t) and bottom quark (b) on the quark side. The electric charge defines the interaction strength with the EM force. All charged leptons posses an electric charge of -1 elementary charge (e). Whereas up-type quarks (u, c, t) carry a charge of $+^2/_3$ e and down-type quarks (d, s, b) carry a charge of $-^1/_3$ e. For every fermion there exists an antiparticle counterpart with oppsite electric charge and spin. Especially the first generation of fermions constitute to the overwhelming part of matter, where protons and neutrons are build with the u- and d-quarks and electrons as part of atoms.

The force carrying bosons include the photon (γ) for the EM interaction, the $W^\pm$ and Z bosons for the weak interaction and eight gluons with different colour for the strong interaction. The photon is mass- and chargeless, with it coupling to every particle possesing an electric charge. The $W^\pm$ and Z bosons of the weak interaction carry relatively high mass, which is the reason for its narrow interaction range. The weak force acts on every fermion, where the $W^\pm$ bosons couple to the weak isospin and the Z boson couples to the weak hypercharge, a combined value of the electric charge and weak isospin. Gluons, mediating the strong interaction, are massless as well and couple to any particle carrying a colour charge, either quarks or glouns themselves. There are the three base colours red, green and blue with a respective anticolour counterpart. Gluons always carry two colour charges, one base colour and one anticolour, resulting in eight different possible permutations. Quarks carry only one colour charge. Colour confinement states that every stable composite particle has to be colorless, which is the reason for the finite range of the strong interaction. These stable composites are called hadrons and are further split into mesons and baryons. Mesons are colour neutral quark-anitquark pairs. Baryons are colour neutral composites of three quarks. The Higgs Boson, proposed by Peter Higgs in 1964 [**higgs**], was discovered in 2012 in a combined effort of the ATLAS [**atlas_higgs**] and CMS [**cms_higgs**] experiment at the LHC. As a scalar boson it carries spin 0, no electric charge and is the heaviest boson ($m_\mathrm{H} = (125.20 \pm 0.11)\,\mathrm{GeV}$ [**higgs_mass**]). It mediates none of the fundamental forces, but by coupling to it fermions and the $W^\pm$ and Z boson gain their mass.
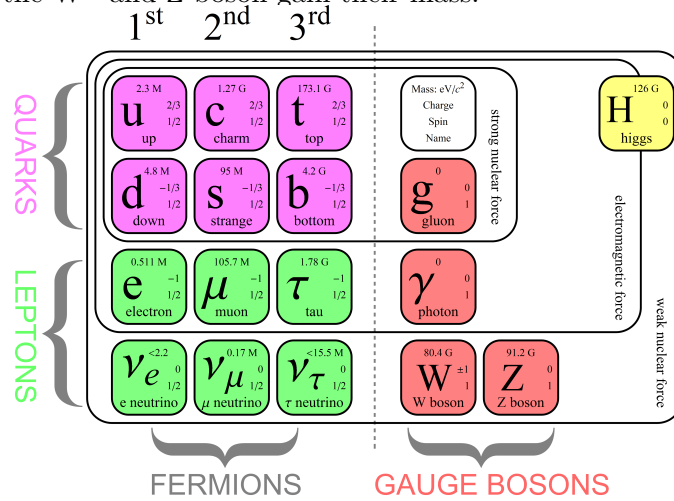

Figure 2.1: The fundamental particles of the Standard Model, showing which forces act on them respectively [4]

2.2 The Top Quark

First postulated by Makoto Kobayashi and Toshihide Maskawa in 1973 and later discovered at Fermilab with the CDF and DØ experiments of the Tevatron collider in 1995 in $p\overline{p}$ collisions, the top quark is the last discovered quark in the SM. As up-type quark in the third generation, it carries the heaviest mass of all quarks at $m_{\rm t} = (172.53 \pm 0.29)\,{\rm GeV}$ (citation), it posseses a large decay width of $\Gamma_t = 1.42^{+0.19}_{-0.15}\,{\rm GeV}$ (citation). A large decay width leads to a short mean life time of $\tau = {}^{\hbar}/_{\Gamma_{\rm t}} \approx 5 \times 10^{-25}\,{\rm s}$. Unlike other quarks, which hadronise due to colour confinement, the top quark decays before hadronisation is possible, due to its short lifetime. The tops properties, like spin information or kinetic properties, are then to be decoded by studying the decay particles, which makes its analysis especially interesting. The top quark decays almost exclusively into a W-boson and a b-quark.

2.2.1 Single top-quark production in the s-channel

The s-channel is one of the electroweak single top-production modes. In the single top-quark s-channel, a top-quark and a bottom anitquark are created from a virtual W-boson, after the annihilation of a quark and antiquark. The s-channel shows a tWb vertex, where the CKM matrix element $V_{\rm tb} \approx 1$ is involved. Therefore the s-channel is a strong probe for the electroweak properties of the top quark. In the LHC, the annihilating particles are predominantly valence up quarks (u) and antidown ($\overline{d}$) from the pool of sea quarks in the colliding protons. The Feynman diagram of the s-channel process at LO is shown in Figure 2.2a.

The parton density function (PDF) is a representation of the probability distrubtion with wich a parton carries a fraction of the momentum of a hadron, denoted by using the *Bjorken x*. $p_i = x p_p$ resembles the momentum fraction the parton i carries from the whole proton momentum p_p. Where a parton is a hadron component, either a quark or gluon. The cross-section $\sigma_{\rm s-chan.}$ of the single top quark s-channel process, is determined using the factorisation theorem of the QCD. By convolving the PDFs of the parton constituents i and j with the cross section $\sigma_{ij \to t\overline{b}}$ of the respective sub-process and then summing over all possible sub-processes, the s-channel cross section is determined.

$$\sigma_{\rm s-chan.} = \sum_{i,j} \int {\rm d}x_i f_i(x_i, \mu_{\rm F}^2) \int {\rm d}x_j f_j(x_j, \mu_{\rm F}^2) \sigma_{ij \to t\overline{b}}(\sqrt{s}, m_t, \mu_{\rm F}, \mu_{\rm R}, \alpha_S).$$

The formular takes in, the centre-of-mass energy $\sqrt{s}$ of the process, the top quark mass m_t, the coupling strength of the strong interaction α_S, as well as the factorisation scale μ_F and the renormalisation scale μ_R, which are set to the energy scale of the process.
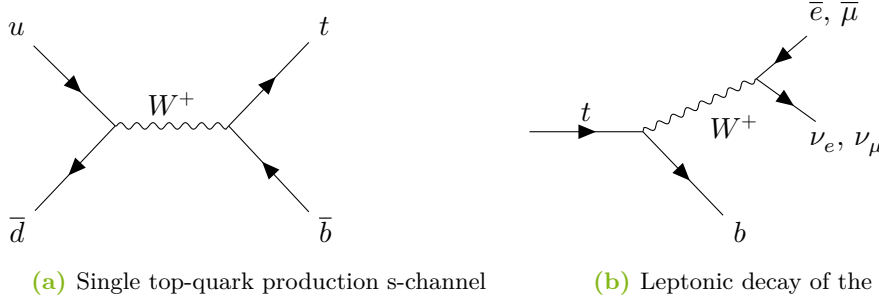
Figure 2.2: Feynman Diagram of the singlte top-quark s-channel production mode and further decay of the top-quark.

2.2.2 Top quark decay

The top quarks decay occurs via the weak interaction, hinted by the resulting decay products consisting of a b-quark and a W-boson. Furhter, the W-boson decays either hadronically $^2/_3$ or leptonically $^1/_3$ of the times. Hadronic decay results into quark pairs, wheresas the leptonic decay emits a lepton and its corresponding neutrino. As there are different color permutations the quarks can carry, the phase space for the hadronic decay is larger, making it more likely than the leptonic decay. During the s-channel analysis only leptonic W-boson decays are selected, as the resulting jets from the hadronic decay are contaminated by multijet background. Since neutrinos cannot be directly detected, the event has to be examined for missing transverse momentum $E_\mathrm{T}^\mathrm{miss}$. If the sum of all transverse momenta of all the outgoing particles, does not add to zero, then a particle has remained undetected and the event has missing transverse momentum $E_\mathrm{T}^\mathrm{miss}$, as prior to the pp collision both beam momenta should cancel out. The leptonic decay mode of the top quark, as looked for in this thesis, is shown in Figure 2.2b.

The searched for signature consist therefore of a charged lepton from the leptonic W-boson decay, missing transverse momentum $E_\mathrm{T}^\mathrm{miss}$ from the undetectable neutrino, and two b-tagged jets, one produced from the $\bar{b}$-quark of the s-channel process itself and one from the b-quark of the top-quark decay. τ leptons have a short lifetime and can thus not be detected, but first and second generation leptons from the τ

decay can be observed. Because of that lepton signature is narrowed down to either an electron or muon.

2.2.3 Background Processes

There are processes with similar signatures in the detector. Differentiating these processes from the signal process of interest is a major task in any analysis. These so called background processes consist predominantly of $t\bar{t}$ production and W+jets production for the single top s-channel analysis. In the LHC experiment $t\bar{t}$ production occurs mostly through gluon-gluon fusion, but with less probability can also happen through quark-pair-annihilation. With a theoretical cross-section of $\sigma_{t\bar{t}}^{\text{Theo.}} = 832^{+20}_{-29}$ pb[**ttbar_cross**], it exceeds every other top quark production mode. The other single top quark production modes can be mistaken for signal as well, but to a lesser degree, since their cross sections are noticeably smaller than $t\bar{t}$ with $\sigma_{t-\text{chan.}}^{\text{Theo.}} = 216.99^{+9.04}_{-7.71}$ pb and $\sigma_{tW-\text{Prod.}}^{\text{Theo.}} = (71.7 \pm 3.8)$ pb. Other minor backgrounds stem from multijet background processes, Z+jets or diboson(WW,WZ,ZZ) production. Figure 2.3 shows the LO Feynman diagrams for $t\bar{t}$ production via gluon-gluon fusion in the s-channel, and the other two single top-quark production modes.
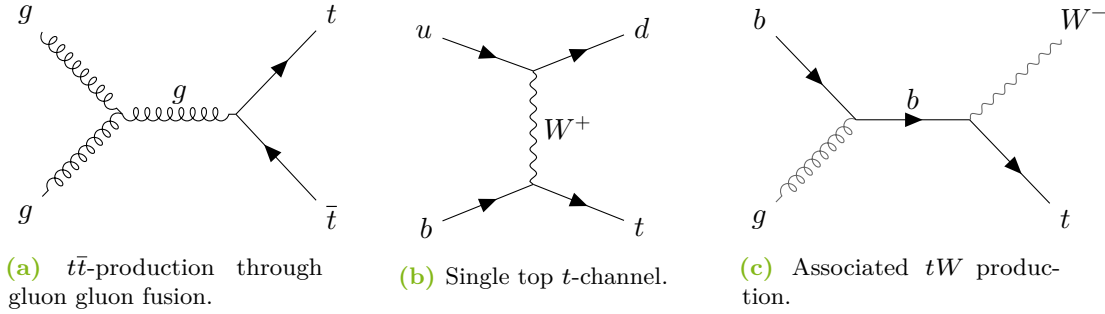

(a) $t\bar{t}$-production through gluon gluon fusion.

(b) Single top t-channel.

(c) Associated tW production.

Figure 2.3: Feynman diagrams at LO for the major background processes in the analysis of the single top quark s-channel production mode.

Not only does the $t\bar{t}$-production mode hold a high cross-section, but the fact that it produces real top-quark decays makes it a difficult background. The two *W*-bosons, resulting from the t-quark and $\bar{t}$-quark decay, again can decay leptonically or hadronically. If both *W*-bosons decay leptonically, the dileptonic final state, can mimic the signal signature if one of the leptons stays undetected. For the semileptonic decay, where one *W*-boson decays leptonically and one hadronically, the final state signature can emulate the signal if only two b-tagged jets get detected. The fully hadronic decay is very unlikely to be mistaken for the signal. Likewise the

single top-quark production mode in the *t*-channel and the associated *tW* production show real top quark decays in their signatures. For the *t*-channel the final state reproduces the signal signature if a b-tagged jet or misidentified lighter quark jet gets associated with the event. In the associated *tW*-production, the *b*-quark turns into a *t*-quark by emitting a *W*-boson. If this *W*-boson decays hadronically and produces a b-tagged jet or a jet that gets misidentified, the final state signature is the same as the signal signature. Provided, the *W*-boson decays leptonically and two b-tagged jets or misidentified jets get associated with the event, the W+jets background mimics the signal. And in the case of multijet background, leptons from heavy flavor decays, electrons from photon conversion or jets misidentified as leptons paired with two associated b-tagged jets or misidentified jets lead to the signal signature.

2.2.4 Previous measurement

- Beschreibe welche Unsicherheiten genau die vorherige Messung verschlechtert

In Figure 2.4 previous measurements of the three different single top-quark production modes at different center of mass energies $\sqrt{s}$ are shown, taken at the ATLAS and CMS experiments at the LHC with data from *pp*-collisions.
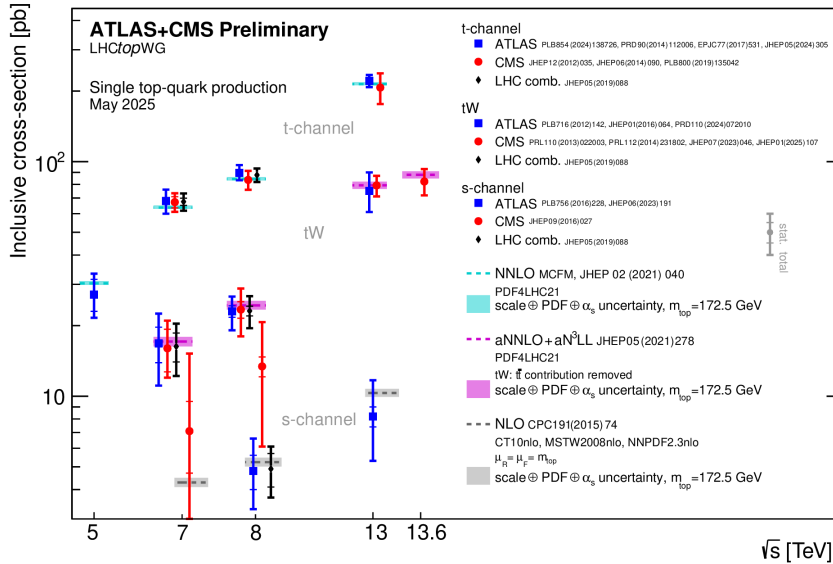

Figure 2.4: Chart of all measurements taken of the three different sinlge top production modes at the ATLAS and CMS experiments [**prev_measure**]

The most recent measurement of the s-channel was done by ATLAS with a center of mass energy of $\sqrt{s} = 13\,\text{TeV}$, with data collected between the years 2015 and 2018, corresponding to the Run 2 dataset at an integrated luminosity of $140\,\text{fb}^{-1}$. The cross section of the measured s-channel resulted in $\sigma_{\text{s-chan}} = 8.2 \pm 0.6(\text{stat.})^{+3.4}_{-2.8}(\text{syst.})\text{pb}$, in comparison to the theoretical estimate of $\sigma_{\text{s-chan}}^{\text{theo.}} = 10.32^{+0.40}_{-0.36}\,\text{pb}$. This is equivalent with an observed (expected) signal significance over the background only hypothesis of $3.3(3.9)\sigma$. The analysis strategy consisted of a preselection and then a split into one signal region and three validation regions, for better modelling of the background processes. To extract the signal strength from the events, a profile likelihood fit was done, with a matrix element method (MEM) discriminant. The limiting factors of the previous measurement where noticeably the systematic uncertainties, where $t\bar{t}$ modelling and signal modelling uncertainties, as well as detector modelling uncertainties, had the biggest impact (Irgendwie muss ich das ja noch zeigen? Wie soll ich da mit der Systematics Tabelle aus dem Paper umgehen?).
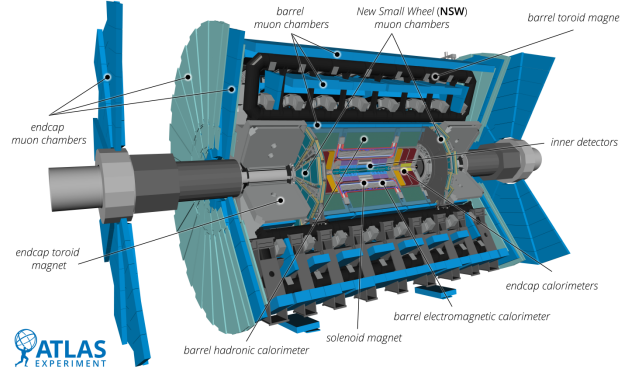
3 The ATLAS detector

Figure 3.1: Schematic overview of the ATLAS Detector and all its subsystems [1]

As a general purpose detector, the ATLAS detector covers a solid angle range of 4 π. The full angular coverage in the beams symmetry plane is granted through its cylindrical design, with a central barrel and two endcaps. It consists of three main subsystems, which are the *Inner Detector* (ID), the *Calorimeter System* and the *Muon Spectrometer* (MS). With the help of a 2 T solenoid magnet, the trajectory of charged particles are bent using the Lorentz force and then reconstructed inside the ID. The calorimeter system consists of an Electromagnetic Calorimeter (ECAL) and Hadronic Calorimeter (HCAL). Inside the ECAL the incoming electrons and photons trigger showers, which ionize parts of the calorimeter and results in energy and direction measurements. Similarly, the HCAL absorbs hadronic jets and triggers hadronic showers, leading to light emissions in the scintillator tubes of the HCAL, from which energy and direction of the jets are determined. As minimal ionizing particles, muons pass all the previously mentioned subsystems and can only be detected in the MS. Here the toroidal magnets in the endcap and barrel parts of the detector bend their tracks and helps in trajectory and charge measurements.

Cartesian coordinates within the LHC are defined as follows: The z-axis is aligned with the beam pipe, the x-axis points to the center of the LHC and the y-axis points upwards to the beam plane. To introduce spherical coordinates, ϕ is used to describe the angle between the y- and x-axis, while θ describes the angle between the y- and z-axis. Lorentz invariance can then be achieved by introducing the pseudorapidity

$\eta = -\ln(\tan\frac{\theta}{2})$. Particle distances within the detector are then defined by the value $\Delta R = \sqrt{\Delta\eta^2 + \Delta\phi^2}$. Transverse momentum is calculated within the cartesian coordinates with $p_\mathrm{T} = \sqrt{p_x^2 + p_y^2}$.

4 Object Definition and Event Selection

4.1 Monte Carlo Samples

In order to study processes in particle physics, signal processes have to be seperated from background processes. Instead of only using recorded data, simulations are done, to better compare these processes with their SM predicitons, via varying assumptions and parameters. In this thesis the single top-quark s-channel production mode is to be examined, with the major backgrounds being $t\bar{t}$-production, single top-quark production in the t-channel, associated tW-production, W+jets and Z+jets production. As multijet background is estimated via fits to data, it is dropped out of consideration. Monte Carlo (MC) simulators are used to reproduce particle events using a Markow Chain process. At LO and NLO, hard scattering events can be calculated using pertubation theory, by calculating the relevant matrix elements (ME). Whereas parton showers (PS) and hadronization due to the strong interaction have to be calculated, utilizing phenomenological models to incorporate the effects of confinement and asymptotic freedom present in QCD. These models use different hadronization models and free parameter, which are tuned using recorded data. As a general purpose MC simulator SHERPA can calculate the hard scattering ME, as well as parton showers and hadronisation. POWHEG BOX V2 can generate hard scattering events up to NLO. PYTHIA 8 models parton shower and hadronisation via the *Lund String model*, typically making use of the *A14* tune. HERWIG 7 calculates parton showers and hadronisation via the *heavy cluster model*. Finally, EVTGEN simulates the decay of heavy-flavour hadrons, especially b and c hadrons. During all simulations a top-quark mass of 172.5 GeV is utilized.

For the nominal single top-quark and antitop-quark s-channel samples, POWHEG simulations combined with PYTHIA are used under the *A14* tune. Heavy-flavour decays are further calculated by EVTGEN.

The t-channel single top-quark and anti-quark processes similarly make use POWHEG and PYTHIA. The leptonic decay of the W-boson from the top-quark decay is enforced and a Breit-Wigner propagator scheme with a fixed top-quark width of 50 GeV is used.

Associated tW production samples are generated with POWHEG interfaced with PYTHIA, while further making use of the diagram removal scheme (citation) to handle interference with $t\bar{t}$ production at NLO. The NNPDF3.0NLO PDF set is used in HERWIG for these samples.

The $t\bar{t}$ production is both simulated with the full-sim and fast-sim detector model, while utilizing the POWHEG generator at NLO with the NNPDF3.0NLO PDF set, combined with PYTHIA. The h_{damp} parameter, which regulates the first gluon emission beyond the Born configuration (Was ist das?), is set to $1.5 \cdot m_{\mathrm{top}} \simeq 258.75\,\mathrm{GeV}$.

For the W+jets samples the SHERPA 2.2.11 version is used, instead of SHERPA 2.2.14. Here SHERPA calculates the matrix elements at NLO accuracy for up to two partons and at LO accuracy for up to five partons, which is combined with parton shower models.

The Drell-Yan production modes of $Z \rightarrow ee$, $Z \rightarrow \mu\mu$, $Z \rightarrow \tau\tau$ are simulated with SHERPA 2.2.11 for the light leptons. For tau decay SHERPA 2.2.14 with the NNPDF3.0NNLO PDF set is utilized. Samples inside different invariant-mass regions, involving a low-mass interval of $(10 < m_{ll} < 40\,\mathrm{GeV})$, is used to improve description of dilepton spectra.

4.2 Object Definition

The signal signature consist of different objects of significance: leptons, either electrons or muons, and their corresponding neutrinos, as well as hadron jets, especially important b-tagged jets. To reconstruct these objects from the detector response a framework for the respective object defintions is to be used.

Electrons are reconstructed from particle tracks in the ID and energy deposits in the ECAL. A measured $p_{\mathrm{T}} > 10\,\mathrm{GeV}$ and $|\eta_{\mathrm{cluster}}| < 2.47$, while deposits in the barrel-end cap transition region $1.36 < |\eta_{\mathrm{cluster}}| < 1.52$ are discarded, are necessary, as well as passing the TightLH and isolation working point, for an electron to be identified as such. Muons require at least a $p_{\mathrm{T}} > 10\,\mathrm{GeV}$ and $|\eta| < 2.5$, while passing the medium quality definition and tight isolation working point. Jets are reconstructed with the anti-k_t algorithm with a radius parameter of $\Delta R = 0.4$. The GN2v01 algorithm, determines if a jet is to be determined as b-tagged.

4.3 Event Selection

With the expected signal signature in mind, a framework for the event selection is used. For single top quark production in the *s*-channel, a charged lepton, either electron or muon, missing transverse momentum E_T^{miss} from the undetected neutrino, and two b-tagged jets are expected. A preselection in the ntuple production inside TOPCPTOOLKIT is utilized. Only events with at least two b-tagged jets with $p_T > 20\,\text{GeV}$, of which at least one must fullfill the 85% working point requirements, and exatly one isolated lepton with $p_T > 28\,\text{GeV}$, survive. The precise event selection is then achieved inside FASTFRAMES, a software tool to further process ntuples and gather histograms from. For this analysis a single signal region (SR) is defined, without any other validation regions. Events inside the signal region encompass two central jets, each in a $|\eta| < 2.5$ range and fulfilling the 77% b-tagging working point. Further transverse momentum requirements are used, where the leading jet has to satisfy $p_T > 40\,\text{GeV}$, while the subleading jet requires $p_T > 30\,\text{GeV}$. Exactly one isolated lepton, either an electron or muon, with $p_T > 30\,\text{GeV}$ has to be included. An additional lepton veto discards all events with an extra lepton with $p_T < 30\,\text{GeV}$. The missing transverse momentum of the undetected neutrino in an event has to fulfill $E_T^{miss} > 35\,\text{GeV}$, while the reconstructed transverse mass of the *W*-boson,

$$m_T^W = \sqrt{2p_T^l E_T^{miss}(1 - \cos\Delta\phi(l, E_T^{miss}))}$$

is required to be $m_T^W > 30\,\text{GeV}$. Another additional jet veto is used, where events with additional jets carrying $p_T > 30\,\text{GeV}$ or additional jets in the forward region ($|\eta| > 2.5$) are rejected. The SR definition with all the event selection cuts used in this analysis is shown in Table 4.1.

Table 4.1: Definition of the event selection for the Signal Region used in this analysis.

	SR
n(e, μ)	== 1 with $p_{\mathrm{T}} > 30\,\mathrm{GeV}$
n(jets)	== 2, in $|\eta| < 2.5$
n($b - tags$)	== 2, @77%, in $|\eta| < 2.5$
Leading jet p_{T}	$> 40\,\mathrm{GeV}$, in $|\eta| < 2.5$
Subleading jet p_{T}	$> 30\,\mathrm{GeV}$, in $|\eta| < 2.5$
Missing transverse energy ($E_{\mathrm{T}}^{\mathrm{miss}}$)	$> 35\,\mathrm{GeV}$
Transverse W boson mass	$> 30\,\mathrm{GeV}$
Additional jets (low p_{T}) veto	No jets with $p_{\mathrm{T}} < 30\,\mathrm{GeV}$
Forward jets veto	No jets with $|\eta| > 2.5$
Additional leptons veto	No extra leptons with $p_{\mathrm{T}} < 30\,\mathrm{GeV}$

s-channel	4139.990 ± 850.839
single top tchan	9334.36 ± 1853.71
single top tW	2619.050 ± 612.957
Z+jets	1654.390 ± 882.368
W+jets	$15\,159.50 \pm 7858.56$
ttbar	$75\,216.7 \pm 18\,753.3$
Total	$108\,124.0 \pm 24\,971.1$

Table 4.2: Yields of the analysis

5 Analysis

5.1 Analysis Strategy

Throughout this analysis, steps are taken to determine the signal strength $\mu_{\text{s}-\text{chan.}} = \sigma_{\text{s}-\text{chan.}}^{\text{measured}}/\sigma_{\text{s}-\text{chan.}}^{\text{theory}}$ of the single top quark s-channel process. This is done via a binned likelihood fit, where a *Deep Neural Network* (DNN) output is used as discriminant value, to descern signal events from background events. Only one signal region, pulled from the event selection in Table 4.1, is defined in this thesis. As systematic uncertainties are the limiting factors in the search for the single top quark s-channel process, the systematics with the biggest impact are further inspected and discussed.

5.2 DNN Model

Especially in studying the single top quark s-channel process, a modern machine learning approach is sensible as the small signal to background ratio ($S/B3.4\%$) [3] makes traditional methods difficult. Therefore a DNN output will be used as the discriminant for a binned likelihood fit. The applied DNN was designed by Niklas Düser as part of his Master's Thesis at the *Technische Universität Dortmund* [2] and makes use of several high-level kinematic variables to descern signal events from background events. For every single particle that gets reconstructed, the kinematic variables $p_{\text{T}}, \eta, \varphi$ and the invariant mass m get included as features for the DNN model. Whereas for particle pairs their pseudorapidity difference $\Delta\eta$ and the difference in azimuthal angle $\Delta\varphi$ between them is incorporated as feature. From the detector measurements of the final state particles, every other particle can be retraced up to the virtal W-boson. First, the final state lepton and corresponding neutrino are reproduced. The neutrino cannot be measured directly via the detector but is inferred via studying the missing transverse momentum $E_{\text{T}}^{\text{miss}}$ of the event and further implying the longitudinal impulse of the neutrino, from the condition that the leptons and the neutrinos momentum squared must equal the invariant mass of the decaying W_{Decay}-boson. With the lepton and neutrino reconstructed, the W_{Decay}-boson of the top quark decay can be solved for. The leading b-tagged jet, of the top quark decay gets measured directly by the detector. With information

about the leading b-jet and the W_{Decay}-boson, the top quark can be reconstructed. From detector measurements, the subleading b-jet from the s-channel process itself gets assessed, and with the reconstructed top quark, the last possible step is to reconstruct the virtual $W_{\text{Prod.}}$-boson. Further the transverse mass of the W_{Decay}-boson defined as $m_{\text{T}}^{\text{W}} = \sqrt{2p_{\text{T}}^l E_{\text{T}}^{\text{miss}}(1 - \cos \Delta\varphi)}$, with p_{T}^l the transverse momentum of the lepton decay product and $\Delta\varphi$ the angle between lepton and neutrino, is included as feature. As well as the transverse mass of the top quark, defined as $m_{\text{T}}^{\text{top}} = \sqrt{E_{\text{T,sum.}}^2 - p_{\text{T,sum.}}^2}$, with the sums of the transverse energies and transverse momenta of the top quarks decay particles, being the lepton, neutrino and b-quark. The scalar sum of the transverse energies of all final-state paricles is called H_{T}, whereas $H_{\text{T,had.}}$ and $H_{\text{T,lep}}$ sum only over the transverse energies of the final state hadrons or leptons respectively. Another set of event shape variables are inferred through the momentum tensor, that encodes the high-levels momentum distributions of the reconstructed objects. Its elements are derived by the formular

$$M_{ij} = \frac{\sum_{k=1}^N p_{k,i} p_{k,j}}{\sum_{k=1}^N p_k^2}, \; i,j \in x, y, z$$

by summing over all final-state particles, where $p_{k,i}$ denotes the i-th component of the k-th final state particle. Through the sorted eigenvalues of the momentum tensor $\lambda_0 > \lambda_1 > \lambda_2$ further event variables are constructed:

$$\text{Aplanarity :} \qquad \mathcal{A} = \frac{3\lambda_2}{2},$$
$$\text{Planarity :} \qquad \mathcal{P} = \frac{3(\lambda_2 + \lambda_1)}{2},$$
$$\text{Spericity :} \qquad \mathcal{S} = \lambda_1 - \lambda_2.$$

The model was trained on both fullsim and fastsim datasets, as well as including single top quark s-channel samples with varying top quark masses for increased statistics. Angular variables are cosine transformed to avoid discontinuities at $\pm\pi$ and variables carrying long tails are log-transformed to compress their dynamic range. All variables are transformed into standardised units, to avoid distortion of variable importance due to their absolute values. Data is split into even and odd samples, only in respect to their event number without taking any other variable feature into consideration. The DNN model outputs a value between 0 and 1, where 1 marks an event as totally corresponding to the signal and 0 marks the event as

background. With the neural network output x as the discriminant, the expected number of events $\lambda_i(\mu, \theta) = \mu \cdot s_i(\theta) + b_i(\theta)$ is used to incorporate the signal strength. Here $s_i(\theta)$ and $b_i(\theta)$ signify the expected signal and background contributions for the i-th bin, which are gathered by putting signal and background events through the DNN model and evaluating the output score x. Systematic uncertainties can influence the seperation. This is considered through the nuisance parameters (NP) θ, which will be affected further through fitting the binned likelihood. The signal strength μ serves then as a scaling factor for the expected signal yields across all bins. The DNNs output is shown in the form of the seperation plot in Figure 5.1a and the combined DNN output histograms of each respective process shown in Figure 5.1b. The event yields given out from the DNN are shown in **??**.

(a) The seperation plot shows the output score of the DNN on the x-axis for the s-channel signal histogram and the sum of the background histograms. Both histograms are normalised. A seperation of 30.1% is achieved, displayed by the observably seperated peaks with yet significant overlap of both distributions.

(b) The combined DNN output for every process of interest in this analysis. Histograms are stacked, where the signal yield is displayed in red on the top of the stack.
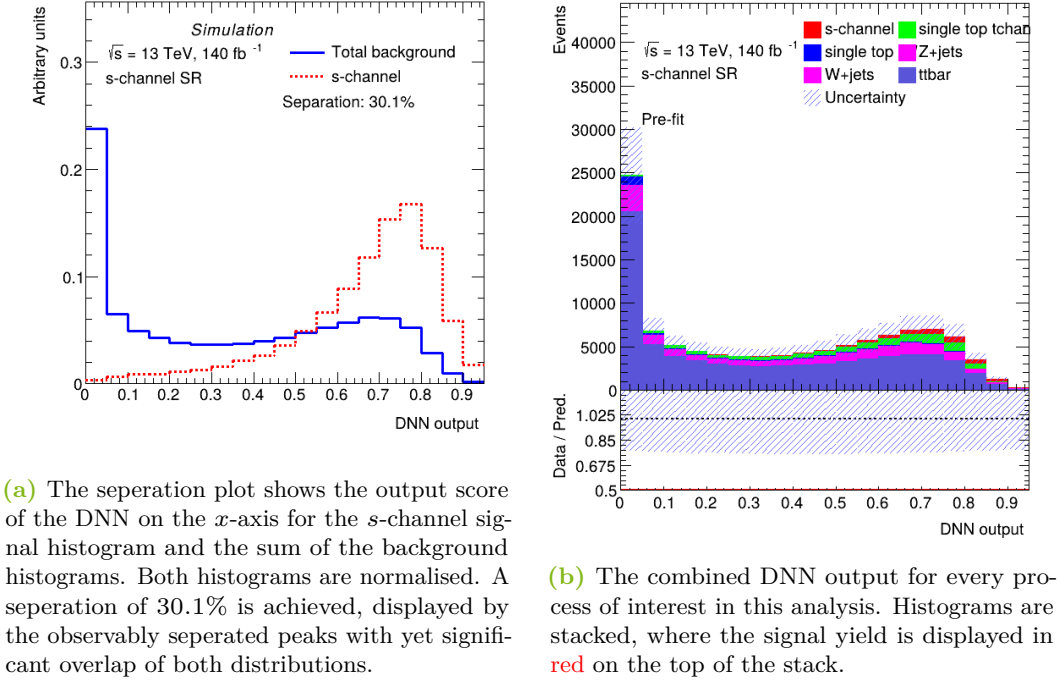
Figure 5.1: The DNNs output is shown with a seperation plot and the combined DNN output for the different processes

5.3 Binned Likelihood Fit

To determine the signal strength, a binned profile likelihood fit is performed with the TRExFitter interface for the HistFactory tool (citation), which modifies the signal

strength and the NPs to maximize the likelihood fuction. The likelihood function states the probability by which an outcome happens in respect of a set of given model parameters. It is used as a framework to determine the signal strength parameter μ and the various NPs of the different systematic uncertainties for which the highest probability is achieved, where the single top quark s-channel process is most likely to occur. As High Energy Particle Physics (HEP) generates large amounts of data, histograms where data is gathered into bins, instead of encompassing each data point individually, are of use. The binning of data also introduces Poisson probabilities into the likelihood as can be seen in the following equation.

$$\mathcal{L}(\mu, \theta) = \prod_{i=1}^{N_{\text{bins}}} \text{Pois}(n_i | \lambda_i(\mu, \theta)) \cdot \prod_{j=1}^{N_{\text{NP}}} \pi_j(\theta_j).$$

The binned likelihood function multiplies the Poisson probabilities $\text{Pois}(n|\lambda)$ in each bin, which state the probability of observing n events under the expectation λ

$$\text{Pois}(n|\lambda) = \frac{\lambda^n e^{-\lambda}}{n!},$$

multiplied with the product of all constraint terms $\pi_j(\theta_j)$ for each NP j. A NP of $\theta_j = 0$ conforms to the nominal prediction made by the simulation, while $\theta_j = \pm 1$ varries the NP in one standard deviation $\pm\sigma$. The constraint term can be modelled as a Gaussian function, where θ_j^0 is set to the nominal value and $\sigma_{\theta_j^0}$ to the uncertainty estimate. One standard deviation estimates for the uncertainties are provided as histograms. NPs are also included as free parameters, called as normalization factors (NF). These are handled as multiplicative factors for signal or background components in the shape of $b(\vec{\theta}, k) = k \cdot b(\vec{\theta})$, which is done for the W+jets process. Statistical uncertainties stemming from the limited number of simulated events are included as NPs γ_i for each respective bin i with a nominal value 1 and modelled as a Poisson term. By maximizing the likelihood function via variaton of the parameters μ and θ_j, their final values are determined by $\hat{\mu}, \hat{\theta} = \underset{\mu, \theta}{\text{argmax}}\, \mathcal{L}(\mu, \theta)$. Typically the negative logarithm of the likelihood function $-\ln \mathcal{L}$ is minimized, as the maximum does not move when taking the logarithm and minimization is often computationally more efficient. The negative log-likelihood (NLL) function is fitted with MINUIT (citation). μ and all NPs can vary while fitting, where μ and the NFs are free-floating, while the NPs are penalized based on their respective uncertainties. If after the fit the NP is changed from the nominal value, the data has pulled the NP. If after the fit the uncertainty of a NP is smaller then the provided uncertainty $\sigma_{\theta_j^0}$, the data achieved a constrainment on the systematic uncertainty provided by the NP. Thus

the binned profile likelihood forms a framework for implementing the DNN output as discriminant and enabling the determination of the signal strength μ and the systematics encoded inside the NPs θ_j

5.4 Systematic Uncertainties

A rough categorisation of the systematic uncertainties yield single top s-channel signal modelling uncertainties, background modelling uncertainties, where the $t\bar{t}$ process is especially studied, and detector modelling uncertainties.

Modelling uncertainties occur because of different choices for ME matching and PS simulation by utilizing different generators and choosing values for special variables, that instruct these generators. For the single top quark s-channel signal process, additional samples were produced varying the $p_{\mathrm{T}}^{\mathrm{hard}}$ to 1, changing ME emissions to be specified by the transverse momentum given by POWHEG when utilized by PYTHIA. This systematic then tests the ME matching descriptions of the hardest emission and further the subsequent PS. Additionaly a sample with HERWIG was produced, assesing uncertainties stemming from the different definition for emission hardness, and choice of parton shower and hadronisation model in the individual generators. Another sample is produced with the same ME and PS models as the nominal samples, but in the fastsim regime to evaluate uncertainties from different detector modelling procedures. Similarly, to attain further precision the for the largest background, futher samples were generated for the $t\bar{t}$ process. Again, instead of PYTHIA, POWHEG is interfaced with HERWIG to study ME matching systematics. Another set of samples with $p_{\mathrm{T}}^{\mathrm{hard}} = 1$ is produced for the $t\bar{t}$ process. Lastly samples where the h_{damp} parameter is increased to $3 \cdot m_{\mathrm{top}}$ from $1.5 \cdot m_{\mathrm{top}}$ are generated, which enables studying of uncertainties related to damping radiation with high p_{T} in the hardest emissions.

Additionaly to the ME and PS matching systematic uncertainties, each background process carries uncertainties in their cross-section. For the single top quark production modes an uncertainty of 6% is set. The W+jets and Z+jets background processes are estimated to have an cross-section uncertainty of 50%. As $t\bar{t}$ does have the biggest yield, it is sensible to let its cross-section uncertainty be modelled as a free floating normalisation factor.

The detector modelling uncertainties in this study encompass one-sided and two-sided systematics, where two-sides systematics entail an up and down variation for the positive and negative pull of each respective uncertainty. One-sided systematic uncertainties entail two systematics for the missing transverse momentum $E_{\mathrm{T}}^{\mathrm{miss}}$, which parametrise the Track Soft Term (TST) resolution in parallel and perpendicular

components. Two-sided systematics are more numerous. The luminosity uncertainty is given as 0.83%. Jet uncertainties come in form of jet energy resolution (JER), jet vertex tagger (Jvt) and jet energy scale (JES) uncertainties. JER uncertainties containt effects of noise and campaign difference pre-recommendations, effects from the difference of data and simulation gathered from the MC20 campaign, and various NP modelling uncertainties. For Jvt two different efficiency uncertainties are included. The JES is effected by jet flavour composition and response, b-jet energy scale, various NP modelling effects on a detector, modelling or mixed level. Further, the effect of pile-up, punch through and jet η intercalibration on the JES are included, as well as different pre-recommendations for different further effects on the JES. Many uncertainties for the effect of flavour tagging are considered, especially for b- and c- tagging. Besides jet uncertainties, effects of uncertainties on the electron and muon modelling are taken into account, as well as the effect of pile-up reweighting. Uncertainties for the single top quark s-channel signal and $t\bar{t}$ background modelling stem additionaly from renormalisation and factorisation effects, moreover initial and final state radiation modelling uncertainties are regarded.

In order to achieve independence from statistical fluctuations, the systematics distributions are smoothed. For uncertainties containing an up and down variation, two-sided symmetrization is done. The up and down variation for each respective bin i consists therefore of the mean of both given by $\pm\frac{n_i^{\mathrm{up}}-n_i^{\mathrm{down}}}{2}$. Uncertainties with only an up or down variation undergo one-sided symmetrisation, in which the the existing variation is mirrored for the missing variation.

5.5 Results

After fitting the NLL onto the Asimov Dataset (ich muss nochmal erklären was ein Asimov Datensatz ist), the signal strength results in $\mu_{\mathrm{s-chan.}} = 1^{+0.25}_{-0.20}$. The DNNs output is therefore still consistent with the SM prediction, even after incorporating several more systematic uncertainties into this analysis, as where considered in Niklas' work. From the fit the NPs influences on the signal strength are now accessible. The ranking plot sorts the NPs, with the most influential NP shown on the top of the plot, based on their influence on the signal strength. The pre-fit impact of a NP is determined by calculating the shift in the signal strength between the nominal fit and a fit where the respective NP is fixed to the value $\hat{\theta} \pm \Delta\theta$. Here $\Delta\theta = 1$, which resembles the pre-fit uncertainty of the NP parameter of one standard deviation σ as used in the constraint term. For the post-fit impact a nominal fit and a fit where the NP is fixed with the value $\hat{\theta} \pm \Delta\hat{\theta}$ is compared. $\Delta\hat{\theta}$ describes the uncertainty of the NP after the fit, with $\hat{\theta}$ being the value for the respective NP

maximizing the likelihood function. The ranking plot for this analysis is displayed in Figure 5.2
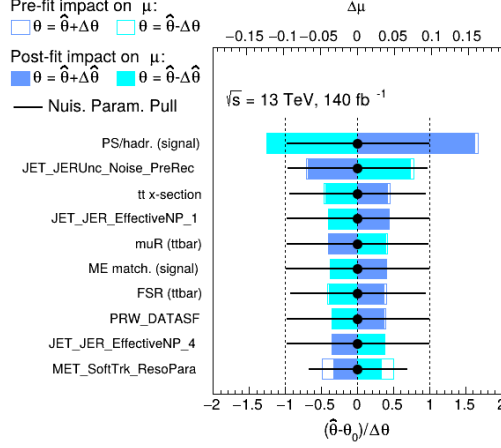

Figure 5.2: The ranking plot sorts the NPs from top to bottom regarding their influence on the signal strength.

The ranking plot reveals that the dominant uncertainty originates from the PS and hadronisation modelling of the single top quark s-channel process. This is expected, since the hadronic signature of the signal consists only of two *b*-tagged jets, whose correlation depend strongly on the modelling of hard emissions and subsequent showering. Furthermore, the features with the greatest impact on the DNNs output are the leading and subleading jets transverse momenta, explaining the strong correspondance to the PS and hadronisation modelling uncertainty. On the detector level the jet energy resolution uncertainties, given by noise pre-recommendation uncertainty and the effective NP 1 uncertainty, have a significant effect on the jet reconstruction and moreover on the jets momenta. Following, is the theoretical prior for the $t\bar{t}$ cross-section uncertainty and the μ_R uncertainty for the $t\bar{t}$ process. Since $t\bar{t}$ is the major top quark production mode and the major background in this analysis, the background modelling uncertainties show a significant impact. The small signal to backround ratio of the single top-quark s-channel process and the large cross-section of the $t\bar{t}$ process explain the sensitivity on the signal strength. Especially the renormalisation uncertainty described by μ_R effects the QCD emissions from the $t\bar{t}$ background, corresponding to alteriations in the kinematic variables of the background signature. In combination with the high sensitivity of the DNN to these high-level kinematics, this explains its large impact. Ratio plots of these NPs effects in contrast to the nominal prediction are displayed in Figure 5.3.

The impact of the overall uncertainties are diminished by the DNN model in comparison the the MEM method used in the previous measurement. This is

(a) PS and hadronisation modelling uncertainty for the signal process.

(b) Jet Energy Resolution Noise pre-recommendation uncertainty for the signal process.

(c) Prior cross-section uncertainty for the $t\bar{t}$ background process.

(d) Jet Energy Resolution effective NP 1 uncertainty for the signal process.

(e) Uncertainty for the renormalisation factor μ_{R} for the $t\bar{t}$ background process.

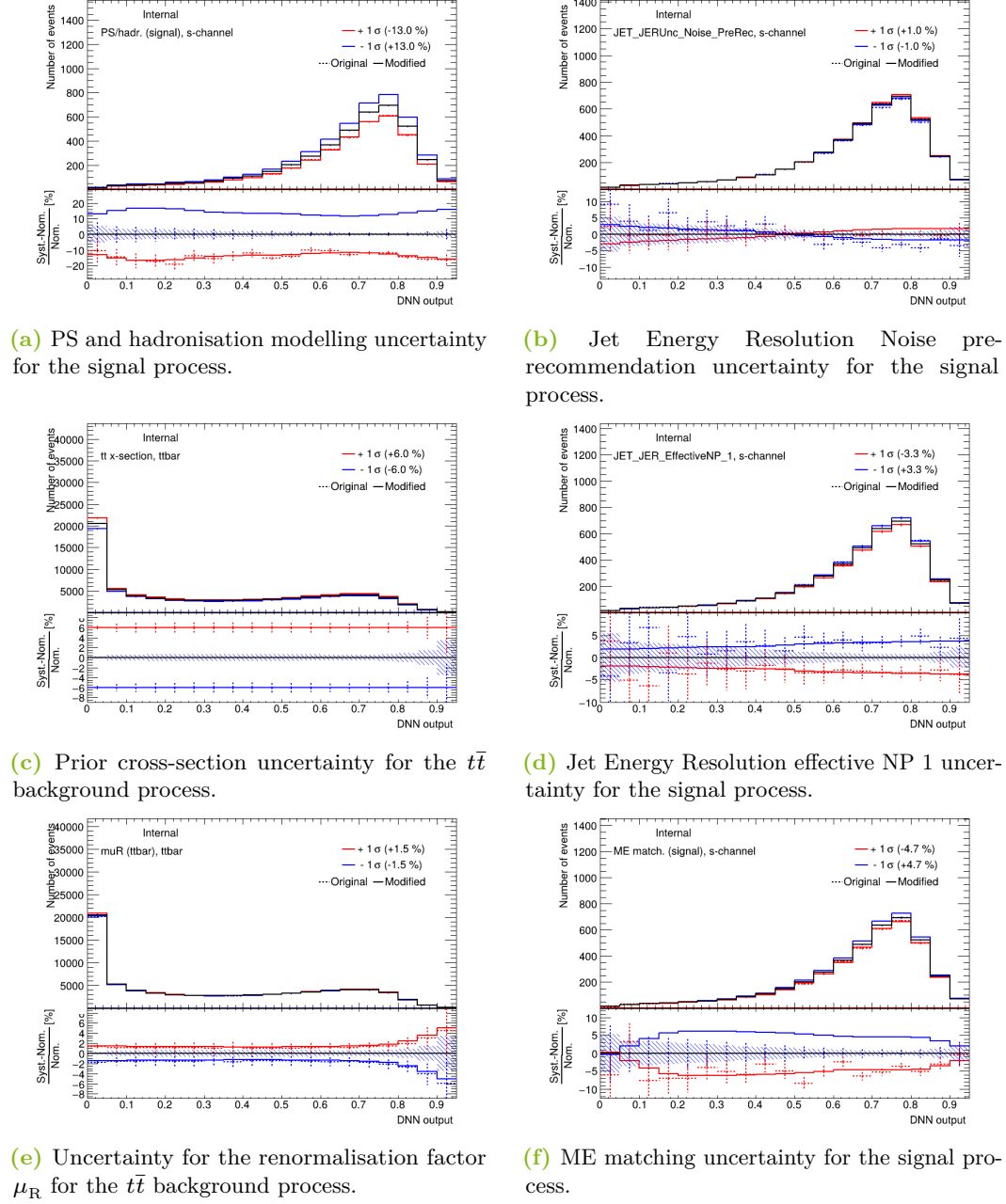**(f)** ME matching uncertainty for the signal process.

Figure 5.3: Ratio plots for the six uncertainties with the biggest impact on the signal strength in this analysis.

displayed in Table 5.1, where the procentual impact of the systematics grouped by categories are displayed. These were determined similarly to the single impacts on shown in the ranking plot. Here the whole set of NPs corresponding to a category are fixed while fitting and then compared to full fit.

Table 5.1: Observed impact of the uncertainties on the measured signal strength of the single top quark s-channel process grouped into categories.

Systematic	Previous measurement: $\frac{\Delta\mu}{\mu}[\%]$	Current measurement $\frac{\Delta\mu}{\mu}[\%]$
Signal Modelling	$+18/-8$	$+6/-6$
Jet Energy Resolution	$+18/-12$	$+11/-9$
Jet Vertex Tagger	$-$	$+1/-1$
Jet Energy Scale	$+18/-13$	$+5/-4$
Flavor Tagging	$+12/-10$	$+4/-4$
Luminosity	$+4/-3$	$+1/-1$
Pile-up Reweighting	$+5/-3$	$+4/-3$

6 Summary and Outlook

A study of the effects of the systematic uncertainties on the signal strength $\mu_{\text{s-chan.}}$ of the single top quark s-channel process was done, as previous measurements were limited by them. For this, simulations based on data of the Run2 dataset, taken between 2015 - 2018 at $\sqrt{s} = 13\,\text{TeV}$ measured with the ATLAS detector, were used. Only the leptonic decay mode of the W-boson from the top quark decay was regarded, leading to a signal signature consisting of one lepton, its corresponding neutrino inferred through the measurement of missing transverse momentum $E_{\text{T}}^{\text{miss}}$, and two b-tagged jets. In this study a single signal region was regarded. As statistical method a binned profile likelihood fit was performed on an Asimov dataset, where the output of a Deep Neural Network was used as discriminant variable. The measured singal strength resulted in $\mu_{\text{s-chan.}} = 1^{+0.25}_{-0.20}$. The uncertainties with the biggest impact on the signal strength were further discussed. These contained the PS and hadronisation modelling of the single top quark s-channel signal process, JER uncertainties on the detector level and background modelling uncertainties for the major background, being the $t\bar{t}$ process.

- keine control regions

- fake estimate

- anderer b-tagging working point

- welche systematics nochmal besser anschauen

A Appendix

Hier könnte ein Anhang stehen, falls Sie z. B. Code, Konstruktionszeichnungen oder Ähnliches mit in die Arbeit bringen wollen. Im Normalfall stehen jedoch alle Ihre Resultate im Hauptteil der Bachelorarbeit und ein Anhang ist überflüssig.

Bibliography

[1] Riccardo Maria Bianchi and ATLAS Collaboration. "ATLAS experiment schematic or layout illustration." General Photo. 2022. URL: https://cds.cern.ch/record/2837191.

[2] Niklas Düser. *Search for single top quark production at ATLAS using Deep Neural Networks and Graph Neural Networks.* Master's Thesis. Sept. 2025.

[3] Pienpen Seema et al. *Search for single top-quark production in the s-channel in proton-proton collisions at $\sqrt{s} = 13$ TeV.* Tech. rep. Geneva: CERN, 2010. URL: https://cds.cern.ch/record/2706904.

[4] Nicola Serra. *Standard Model.* 2025. URL: https://www.physik.uzh.ch/groups/serra/StandardModel.html.

Eidesstattliche Versicherung

(Affidavit)

_____   _____
Name, Vorname   Matrikelnummer
(surname, first name)   (student ID number)

☐ Bachelorarbeit   ☐ Masterarbeit
(Bachelor's thesis)   (Master's thesis)

Titel
(Title)

_____

_____

_____

Ich versichere hiermit an Eides statt, dass ich die vorliegende Abschlussarbeit mit dem oben genannten Titel selbstständig und ohne unzulässige fremde Hilfe erbracht habe. Ich habe keine anderen als die angegebenen Quellen und Hilfsmittel benutzt sowie wörtliche und sinngemäße Zitate kenntlich gemacht. Die Arbeit hat in gleicher oder ähnlicher Form noch keiner Prüfungsbehörde vorgelegen.	I declare in lieu of oath that I have completed the present thesis with the above-mentioned title independently and without any unauthorized assistance. I have not used any other sources or aids than the ones listed and have documented quotations and paraphrases as such. The thesis in its current or similar version has not been submitted to an auditing institution before.

_____   _____
Ort, Datum   Unterschrift
(place, date)   (signature)

Belehrung:	**Official notification:**
Wer vorsätzlich gegen eine die Täuschung über Prüfungsleistungen betreffende Regelung einer Hochschulprüfungsordnung verstößt, handelt ordnungswidrig. Die Ordnungswidrigkeit kann mit einer Geldbuße von bis zu 50.000,00 € geahndet werden. Zuständige Verwaltungsbehörde für die Verfolgung und Ahndung von Ordnungswidrigkeiten ist der Kanzler/die Kanzlerin der Technischen Universität Dortmund. Im Falle eines mehrfachen oder sonstigen schwerwiegenden Täuschungsversuches kann der Prüfling zudem exmatrikuliert werden. (§ 63 Abs. 5 Hochschulgesetz - HG -).	Any person who intentionally breaches any regulation of university examination regulations relating to deception in examination performance is acting improperly. This offense can be punished with a fine of up to EUR 50,000.00. The competent administrative authority for the pursuit and prosecution of offenses of this type is the Chancellor of TU Dortmund University. In the case of multiple or other serious attempts at deception, the examinee can also be unenrolled, Section 63 (5) North Rhine-Westphalia Higher Education Act (*Hochschulgesetz, HG*).
Die Abgabe einer falschen Versicherung an Eides statt wird mit Freiheitsstrafe bis zu 3 Jahren oder mit Geldstrafe bestraft.	The submission of a false affidavit will be punished with a prison sentence of up to three years or a fine.
Die Technische Universität Dortmund wird ggf. elektronische Vergleichswerkzeuge (wie z.B. die Software „turnitin") zur Überprüfung von Ordnungswidrigkeiten in Prüfungsverfahren nutzen.	As may be necessary, TU Dortmund University will make use of electronic plagiarism-prevention tools (e.g. the "turnitin" service) in order to monitor violations during the examination procedures.
Die oben stehende Belehrung habe ich zur Kenntnis genommen:	I have taken note of the above official notification:*

_____   _____
Ort, Datum   Unterschrift
(place, date)   (signature)

***Please be aware that solely the German version of the affidavit ("Eidesstattliche Versicherung")
for the Bachelor's/ Master's thesis is the official and legally binding version.**